

Chapter 4

Analysis of Effect of Oblateness of Smaller Primary on the Evolution of Periodic Orbits

In chapters 2 and 3 we have considered Sun–Saturn system in which actual oblateness of Saturn is taken into account. We have analyzed the effect of solar radiation pressure on Sun centered periodic orbits and Saturn centered periodic orbits in chapter 2, whereas in chapter 3 we have done the stability analysis for f family periodic orbits under the perturbation of solar radiation pressure.

In this chapter we have analyzed family of periodic orbits around both primaries for two systems – Sun–Mars and Sun–Earth systems – using Poincaré surface of section (PSS) technique. During this study effects of oblateness of smaller primary on these orbits are analyzed. It is observed that oblateness of smaller primary has substantial effect on period, shape, size and position of orbits in the phase space. Since these orbits can be used for the design of low energy transfer trajectories, perturbations due to planetary oblateness has to be understood and should be taken into consideration during trajectory design. Periodic orbits, with three-loops for $A_2 = 0.0001$, have been analyzed in detail for its stability.

4.1 Introduction

A low-energy transfer trajectory [Koon et. al.(2001)] is a trajectory in space that allows spacecraft to change the existing orbits using very small amount of fuel in comparison with Hohmann transfer orbit. To construct low-energy transfer trajectories, we require periodic orbits of spacecrafts around both primary bodies. Space agencies are trying to place telescopes into deep space like NASA's Terrestrial Planet Finder and ESA's Darwin project, to find Earth-like planets around other stars exhibiting life. In order to perform space mission to explore different aspects of far away objects, it is required to determine special types of orbits that cannot be found by classical approaches.

However, it is to be noted that the classical approaches to spacecraft design are like Hohmann transfer for Apollo Moon landings and swing bys of outer planets for voyager. But these missions were costly in terms of fuel. A very high fuel requirement for space missions may cause it infeasible. A new class of low energy trajectories has been introduced recently in which low fuel burn is required to transfer the trajectory from initial position to the targeted final position. A proper understanding of low-energy trajectory can be seen in [Koon et. al.(2011)].

Study of orbits of bodies in RTBP has been described in detail by [Szebehely (1967)]. Because of the non-linear nature of the equations of motion involved in the study of the system, analytical methods may not give illuminating insights into the solution. So, PSS is widely used for finding the orbits of the infinitesimal particle (spacecraft) and analyzing periodic, quasi periodic and chaotic orbits. Solar system dynamics by [Murray and Dermot (1999)] provide a detailed analysis of periodic orbits using PSS technique.

As per Kolmogorov-Arnold-Moser (KAM) theory (Moser, 1966), a fixed point on the Poincare surface of section represents a periodic orbit in the rotating frame, and the closed curves around the point correspond to the quasi-periodic orbits. [Dutt and Sharma (2010)] have analyzed the PSS for Earth-Moon system without considering any perturbation. [Dutt and Sharma (2011a)] also have analysed Sun-Mars system by incorporating perturbations due to solar radiation. They have identified periodic, quasi-periodic solutions and chaotic regions from the PSS. Similar studies have been made by [Safiya Beevi and Sharma (2011)] for Saturn-Titan system. They have

studied perturbation due to oblateness of Saturn in the Saturn–Titan system. [Dutt and Sharma(2012)] have analyzed the \mathbf{f} family orbits around smaller primary under RTBP for 14 systems under ideal conditions.

Recently, [Pathak et. al. (2016a)] have done analysis of Sun and Saturn centered periodic orbits with solar radiation pressure and oblateness and found that there is a substantial effect of solar radiation pressure on position and geometry of secondary body’s orbit. [Pathak and Thomas(2016b)] have studied \mathbf{f} family periodic orbits and their stability for Sun–Saturn system with perturbation. In their study Sun was taken as a source of radiation and Saturn was considered as an oblate spheroid. By taking the actual coefficient of oblateness for Saturn and different values of solar radiation pressure, the \mathbf{f} family orbits have been analyzed in detail.

Periodic orbits of spacecraft around two primaries are used to construct low energy trajectory. [Stromgren (1935)] has established three classes with orbits around both primaries depending on motion of spacecraft is prograde or retrograde in the rotating system as well as in fixed system. In this chapter we have analyzed periodic orbits around both primaries with retrograde motion in rotating system and analyzed periodic orbits having number of loops from 1 to 5 for different pairs of oblateness coefficient A_2 and Jacobi constant C for Sun–Mars and Sun–Earth system. It has been found that A_2 and C has substantial effect on the position, shape and size of the orbits and hence must be considered during low energy trajectory design.

4.2 Results and discussion

We shall consider two systems, the Sun–Mars system and the Sun–Earth system. The mass of Sun, Earth and Mars considered in the study are 1.9881×10^{30} kg, 5.972×10^{24} kg and 6.4185×10^{23} kg, respectively, [Dutt and Sharma (2010)]. Thus, for the Sun–Earth and Sun–Mars systems, mass factor μ are 0.000003002 and 0.0000003212 respectively. Equatorial and polar radii of Earth are 6378.1 km. and 6356.8 km. and that of Mars are 3396.2 km. and 3376.2 km., respectively. The distance between Sun and Earth is taken as 149,600,000 km. and distance between Sun and Mars is 227,940,000 km. So, oblateness coefficients calculated from Equation (1.4.19) for Sun–Earth and Sun–Mars systems have values $A_2 = 2.42405 \times 10^{-12}$

and $A_2 = 5.21389 \times 10^{-13}$ respectively. Equations (1.4.12) to (1.4.16) are equations of motion of secondary body under the Sun–Mars and Sun–Earth systems. Throughout this chapter value of q is taken as 1. In other words, effect of solar radiation pressure is not taken into account. But A_2 is taken as variable to study the effect of oblateness on this family of orbits.

In order to study the effect of oblateness on periodic orbit around both primaries, we take different values of oblateness that can make observable changes in different parameters. For a given A_2 , selection of C is not arbitrary. Using equation (1.4.21) we can obtain maximum value of C as explained in chapter 3. Value of C in the range, thus, determined is the admissible value of C .

Table 4.1 and Table 4.2 show range of admissible values of C for Sun–Mars and Sun–Earth systems. It can be observed that for both the systems as oblateness increases, admissible range of C increases. But this increment is larger for Sun–Earth system than Sun–Mars system. So, we can say that as mass factor μ increases, effect of oblateness increases and due to that admissible range of C increases.

For simplicity in writing the head rows of Table 4.1 and 4.2, oblateness, maximum value of C , value of C greater than maximum value of C , lower limit of excluded region, upper limit of excluded region and size of the excluded region are denoted by A_2 , C_M , C , LER , UER and SER respectively.

We have studied the effect of oblateness on the location and period of Sun–Mars system for different values of Jacobi constant C using PSS. Figure 4.1 shows PSS constructed for Sun–Mars system when (A_2, C) is $(0.0005, 2.93)$ by taking value of x from the interval $[0.8, 1]$ with interval of x difference as 0.001. Also, time span $t = 10,000$ time units and interval of time difference is taken as 0.001. So, for each x equations of motion are integrated using Runge–Kutta–Gill method. Each solution is plotted as a point in Figure 4.1. The arcs of PSS are known as islands whose center gives periodic orbit.

In a similar way, we can obtain PSS for Sun–Earth which is shown in Figure 4.2. This PSS is also constructed for the pair (A_2, C) given by $(0.0005, 2.93)$. Our aim is to make a comparative study of the effect of oblateness on different parameters of the orbits of Sun–Earth and Sun–Mars systems using PSS technique. Mass factor

μ of Sun–Earth is greater than μ of Sun–Mars.

Table 4.1: Admissible range of C for Sun–Mars system.

A_2	C_M	C	LER	UER	SER
0.00001	3.000	3.001	0.984	0.999	0.016
0.00005	3.000	3.001	0.984	0.998	0.015
0.00010	3.000	3.001	0.985	0.997	0.013
0.00050	3.001	3.002	0.981	0.995	0.015

Table 4.2: Admissible range of C for Sun–Earth system.

A_2	C_M	C	LER	UER	SER
0.00001	3.000	3.001	0.988	0.992	0.005
0.00005	3.001	3.002	0.978	0.995	0.018
0.00010	3.001	3.002	0.979	0.993	0.015
0.00050	3.002	3.003	0.976	0.990	0.015

For Sun–Mars system, the numerical values of location of periodic orbit and left end (L) and right end (R) of corresponding island for $C = 2.93, 2.94, 2.95, 2.96$ and for oblateness $A_2 = 0.00001, 0.00005, 0.0001$ and 0.0005 are displayed in Table 4.3. It is observed from the table that a change in C in the range $(2.93, 2.96)$ affects the location of the periodic orbits. Oblateness also affects the location of the periodic orbit. Similarly, the effects of C and A_2 in the location of periodic orbits and left end (L) and right end (R) of corresponding island for the Sun–Earth system are studied and the numerical estimates of the changes are displayed in Table 4.4. Size of the island gives stability of the corresponding orbit.

The periodic orbits starting from single-loop to five-loops in the Sun–Mars and Sun–Earth systems for $A_2 = 0.0005$ and $C = 2.93$ are shown in Figures 4.3(a)–(j). It can be observed, from Figure 4.3, that the width of the orbit decreases continuously as the number of loops increases. Further, in all cases the secondary

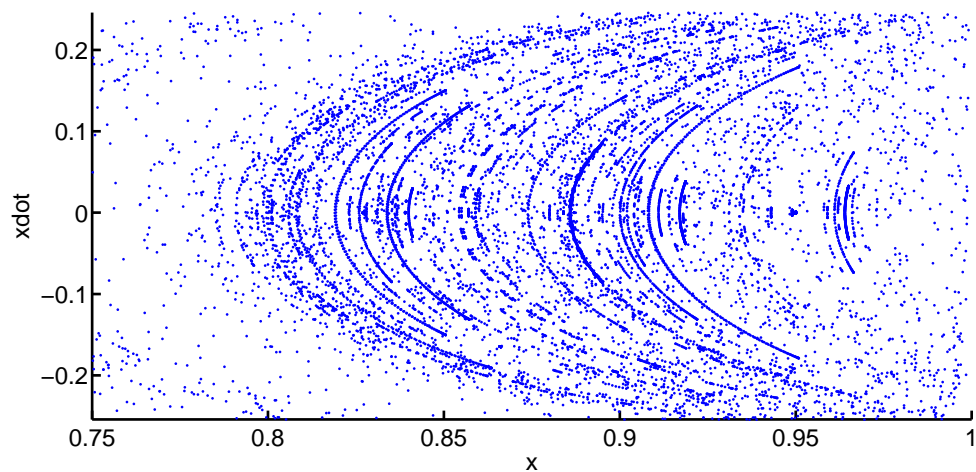


Figure 4.1: PSS for $A_2 = 0.0005$ and $C = 2.93$, for $x = [0.8, 1]$ for Sun-Mars system.

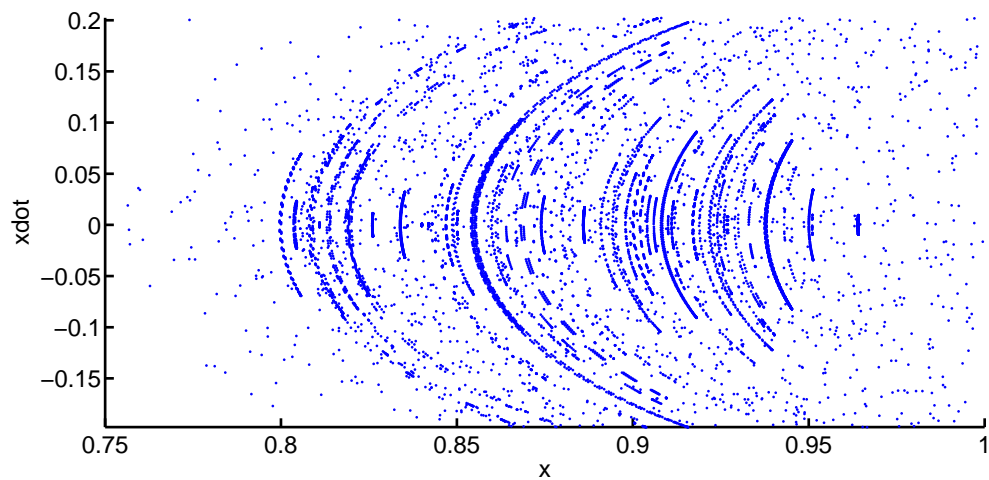
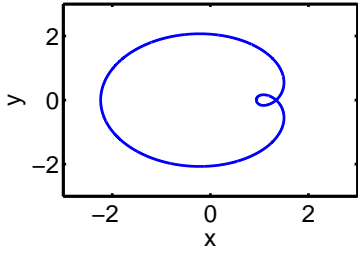
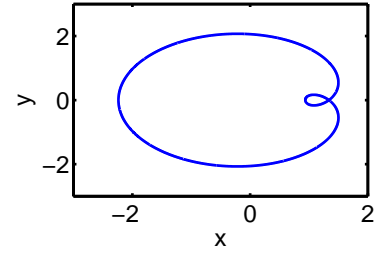


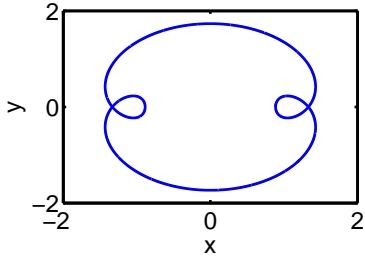
Figure 4.2: PSS for $A_2 = 0.0005$ and $C = 2.93$, for $x = [0.8, 1]$ for Sun-Earth system.



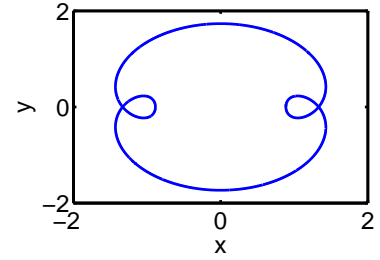
(a) Single-loop orbit with $T = 13$ in Sun-Mars system.



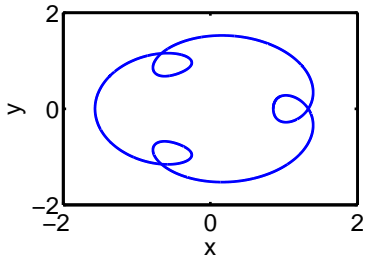
(b) Single-loop orbit with $T = 13$ in Sun-Earth system.



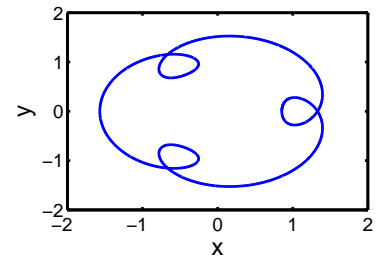
(c) Two-loops orbit with $T = 19$ in Sun-Mars system.



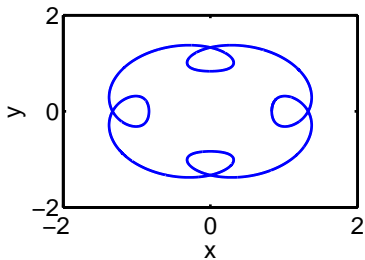
(d) Two-loops orbit with $T = 19$ in Sun-Earth system.



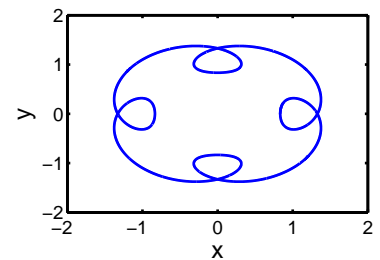
(e) Three-loops orbit with $T = 26$ in Sun-Mars system.



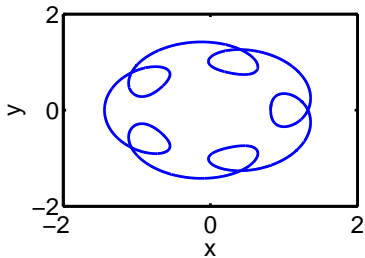
(f) Three-loops orbit with $T = 26$ in Sun-Earth system.



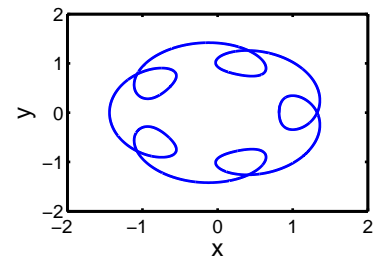
(g) Four-loops orbit with $T = 32$ in Sun-Mars system.



(h) Four-loops orbit with $T = 32$ in Sun-Earth system.



(i) Five-loops orbit with $T = 38$ in Sun-Mars system.



(j) Five-loops orbit with $T = 38$ in Sun-Earth system.

Figure 4.3: Periodic orbits around both primaries for Sun-Mars and Sun-Earth systems when $C = 2.93$ and $A_2 = 0.0005$.

body's (spacecraft's) orbits around the second primary (Mars or Earth) in addition to orbiting both primaries. Further, the secondary body is closest to Mars or Earth in the single-loop closed orbit. Such orbits may be useful in the study of different aspects of both primaries.

In many models available in literature not many closed orbits possess this kind of nature. Further, the position of the orbit in phase space approaches the first primary, namely the Sun as number of loops increases. It can be observed that the period of the orbit remains unchanged due to change in oblateness or mass factor, but period of the orbit increases with increment in number of loops.

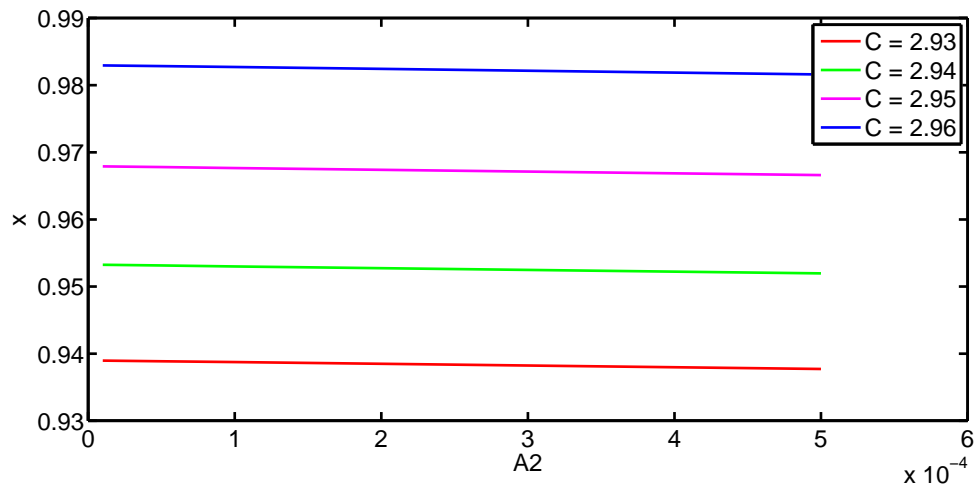


Figure 4.4: Variation in location of single-loop periodic orbit around Sun-Mars system due to oblateness.

We have studied the variation of position of periodic orbits around Sun-Mars and Sun-Earth system due to the variation in oblateness and Jacobi constants C . In Figure 4.4 we have shown the variation of position of closed periodic orbit with single-loop for oblateness in the range (0.00001, 0.0005) for Sun-Mars system corresponding to Jacobi constants $C = 2.93, 2.94, 2.95$ and 2.96 . From Figure 4.4 it is clear that the position of the orbits recedes from Mars, when the oblateness increases and C decreases. Similar kind of conclusion can be drawn from Figure 4.5 for the Sun-Earth system. We have studied the effect of A_2 and C on the position of the orbits having loops varying from 1 to 5 for both Sun-Mars and Sun-Earth systems. The results of these observations for 5-loops closed periodic orbit in both Sun-Mars and Sun-Earth systems are shown in Figure 4.6 and Figure 4.7.

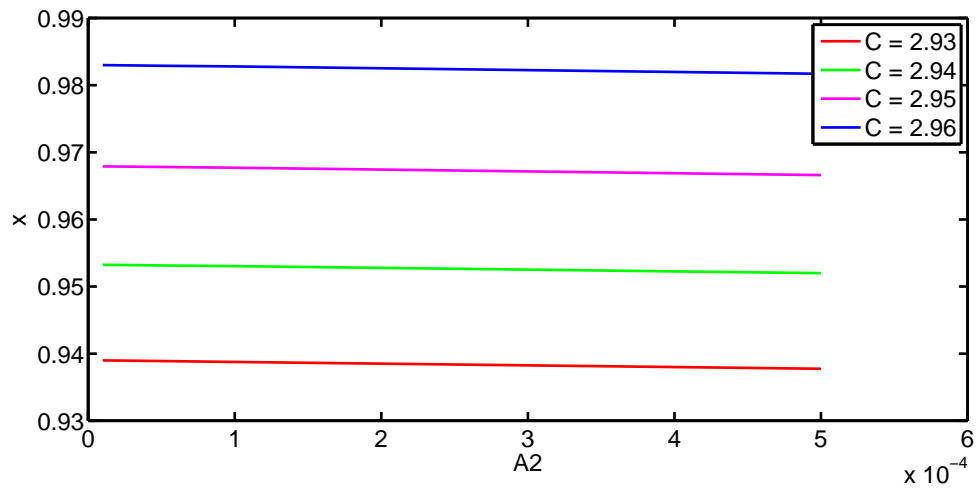


Figure 4.5: Variation in location of single-loop periodic orbit around Sun-Earth system due to oblateness.

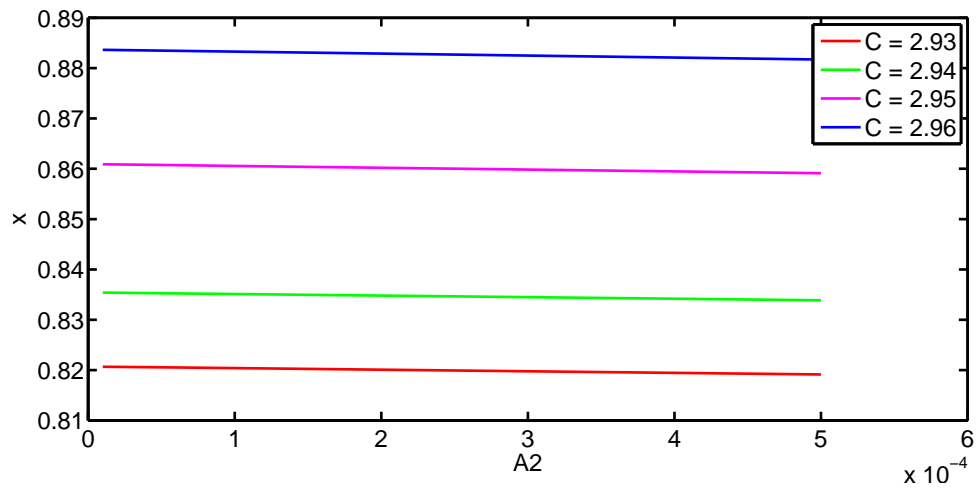


Figure 4.6: Variation in location of five-loops periodic orbit around Sun-Mars system due to oblateness.

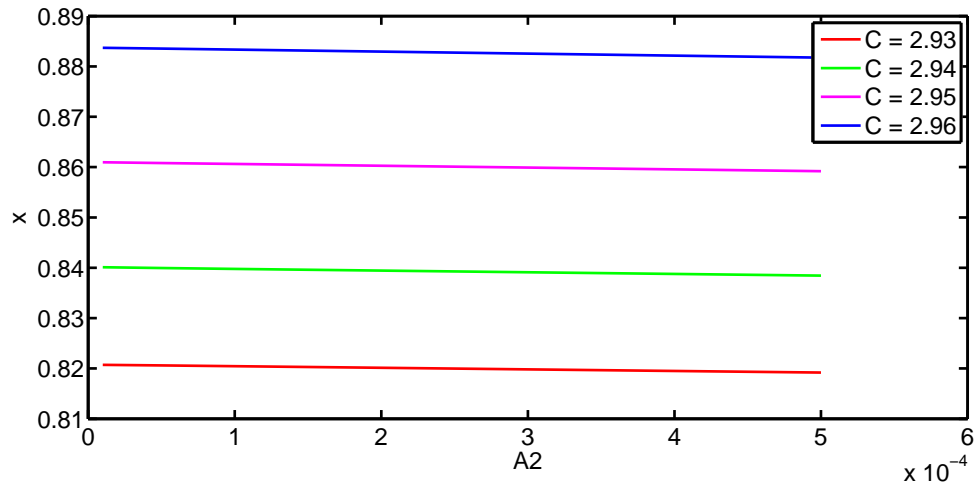


Figure 4.7: Variation in location of five-loops periodic orbit around Sun-Earth system due to oblateness.

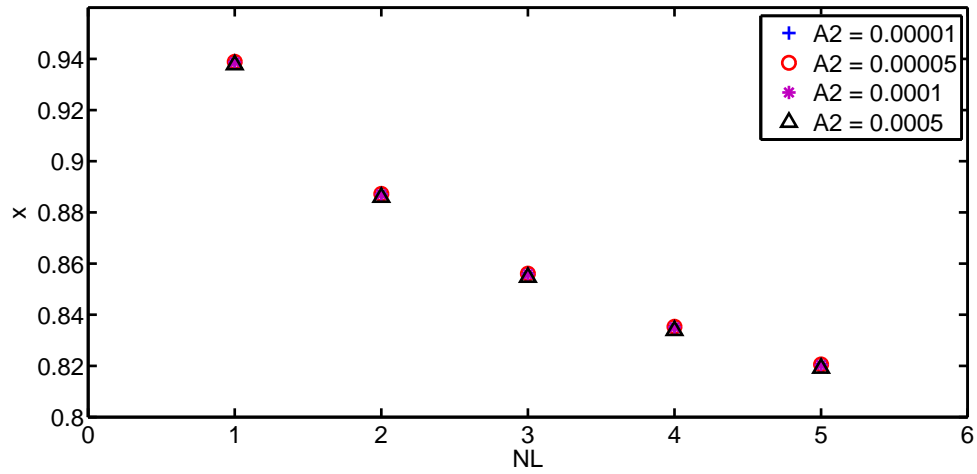


Figure 4.8: Variation in location of periodic orbit of secondary body around Sun and Mars for $C = 2.93$ due to number of loops for different A_2 .

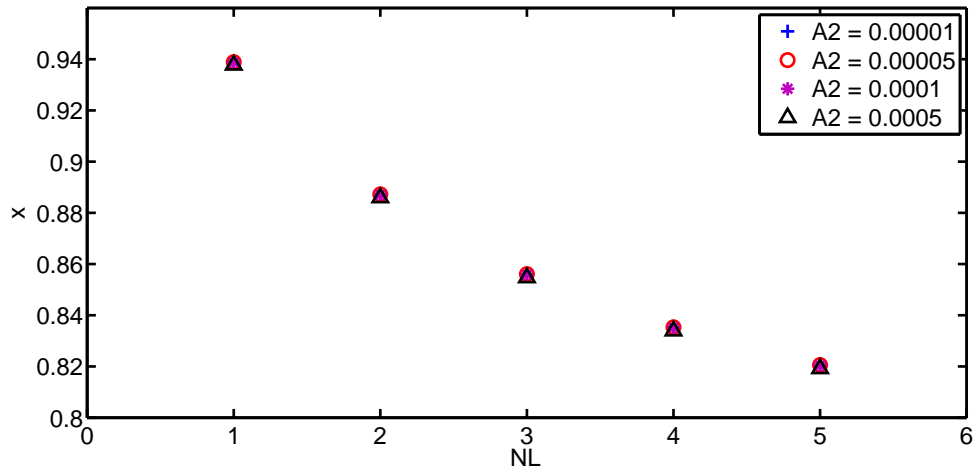


Figure 4.9: Variation in location of periodic orbit of secondary body around Sun–Earth system for $C = 2.93$ due to number of loops for different A_2 .

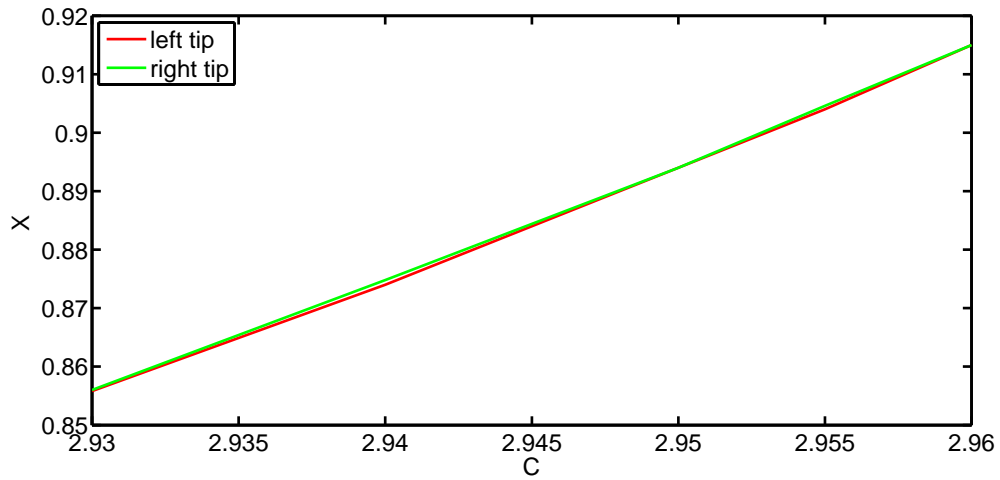


Figure 4.10: Stability analysis for three-loops orbit for Sun–Earth system when $A_2 = 0.0001$.

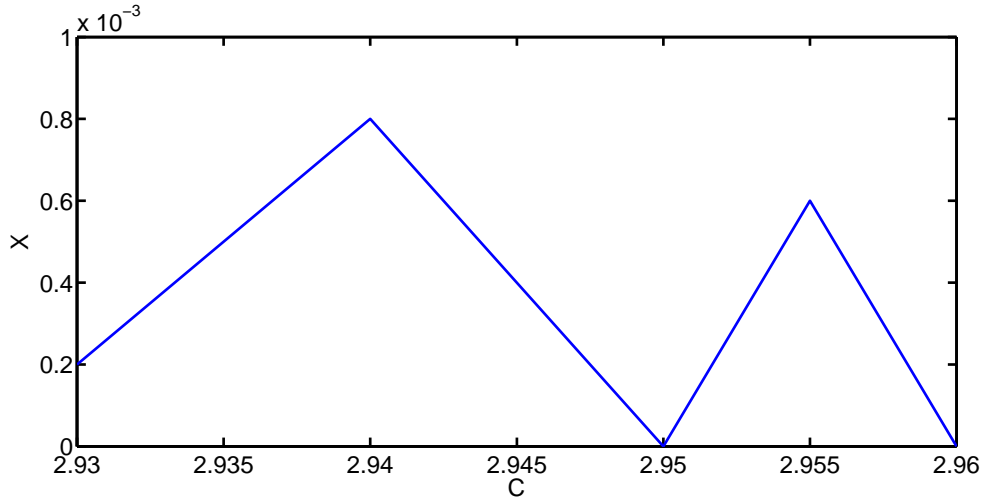


Figure 4.11: Amplitude for three-loops orbit for Sun-Earth system when $A_2 = 0.0001$.

From Figures 4.8 and 4.9, it can be observed that for given oblateness, location of periodic orbit moves away from second primary as number of loops in periodic orbit increase. Also, as oblateness increases, location of periodic orbit moves away from second primary. We have analyzed stability of periodic orbits from loop 1 to 5 for $A_2 = 0.00001, 0.00005, 0.0001$ and 0.0005 . Since stability behavior is similar for all these orbits, the analysis is made for three loops orbit corresponding to $A_2 = 0.0001$. Figure 4.10 shows stability region for $A_2 = 0.0001$ for three loop orbits. The left and right tips of the island are plotted by red and green curves, respectively. From Figure 4.10 it is clear that size of stability region is very small in comparison to f family orbit [Dutt and Sharma(2012), Pathak and Thomas(2016b)]. So, these periodic orbits can be used as a transfer orbits as they are not stable. So, secondary body requires fewer amount of fuel than Hohmann transfer.

Figure 4.11 shows amplitude for three-loops orbit when $A_2 = 0.0001$. It can be observed that there are two separatrices at $C = 2.95$ and 2.96 where stability of the periodic orbit is zero as the size of the island is zero. For $C = 2.94$, we get maximum stability which is 0.0008 . Figure 4.12 shows size of the island for $C = 2.94$ for three-loops orbit when $A_2 = 0.0001$ which is 0.0008 whereas Figure 4.13 shows PSS of first separatrix at $C = 2.95$ which looks like a straight line whereas for f family orbit it is triangular due to third order resonance [Dutt and Sharma(2012), Pathak and Thomas(2016b)]. It can be seen that size of this island is zero. Figure 4.14 shows three-loops orbit corresponding to first separatrix when $A_2 = 0.0001$. Figure 4.15

shows for $C = 2.955$ again size of island increases and it becomes 0.0006, whereas for $C = 2.96$ again size of island becomes zero, which is second separatrix as shown in Figure 4.16. Three-loops orbit corresponding to second separatrix is given in Figure 4.17.

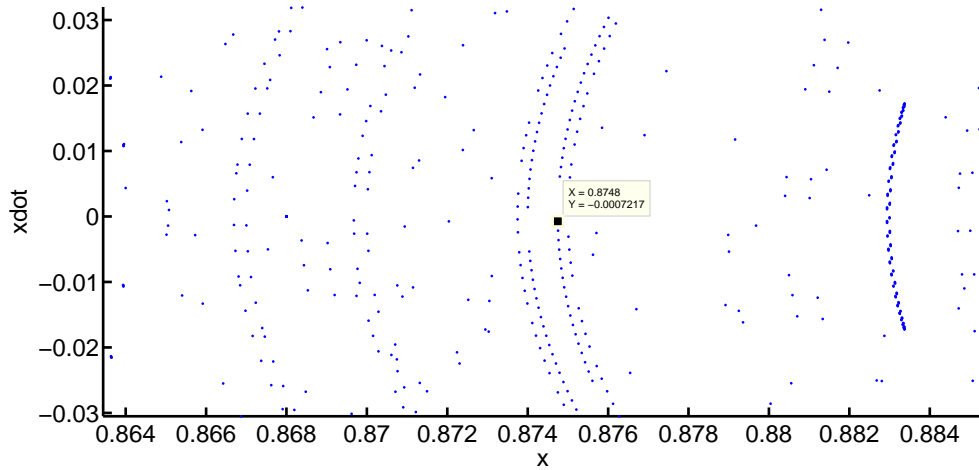


Figure 4.12: Enlarge view of PSS for $C = 2.94$ when $A_2 = 0.0001$.

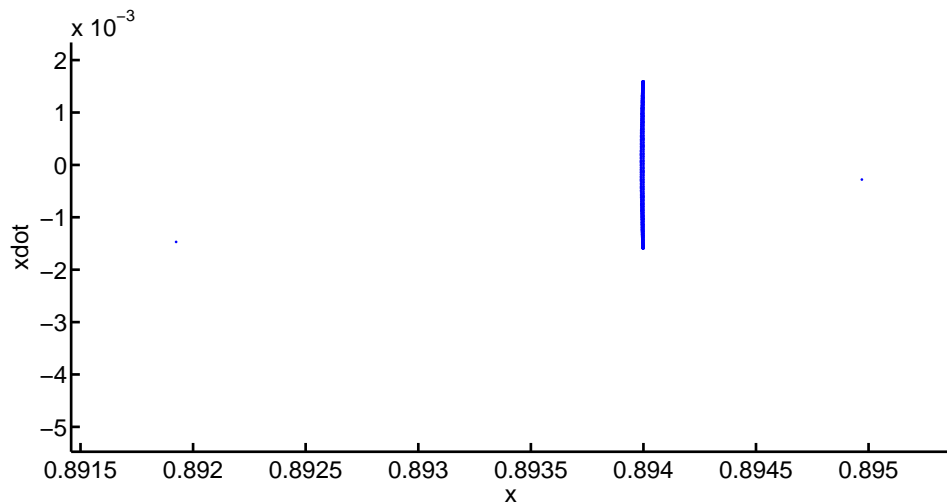


Figure 4.13: Enlarge view of PSS of first separatrix for three-loops orbit for $C = 2.95$ when $A_2 = 0.0001$.

In Table 4.5 initial velocity of secondary body is denoted by V , D_1 and D_2 are the distance of secondary body from Mars and Sun respectively. The unit of V is in $km s^{-1}$, that for D_1 and D_2 is in km. Similar notations are used in Table 4.6 also. In Table 4.6 distance of secondary body from Earth is denoted by D_1 . V can be obtained using Equation (1.5.48). The conversion from units of distance (I) and

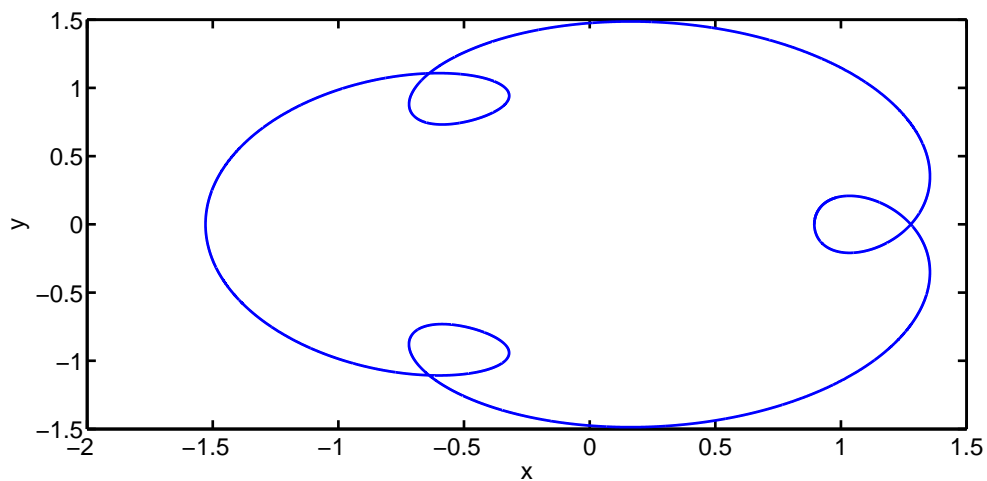


Figure 4.14: Orbit at first separatrix corresponding to $C = 2.95$, $A_2 = 0.0001$ and $x = 0.894$.

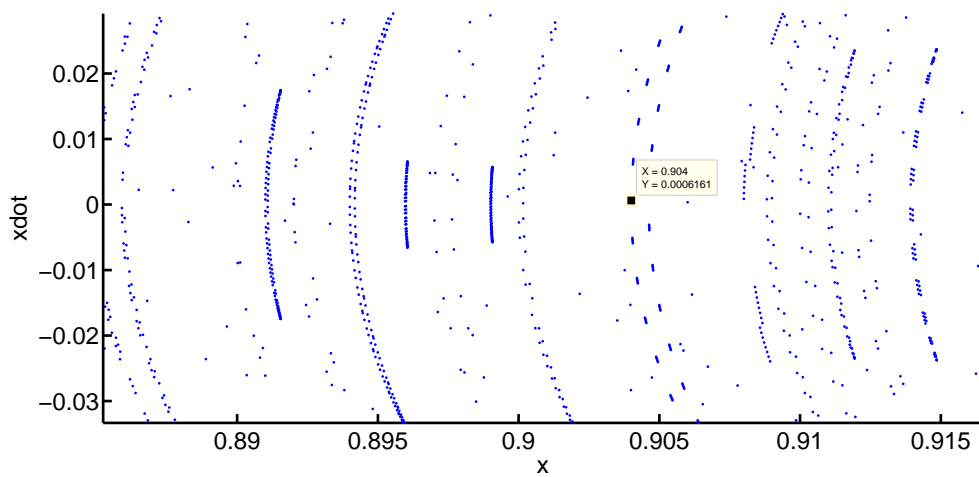


Figure 4.15: Enlarge view of PSS for $C = 2.955$ when $A_2 = 0.0001$.

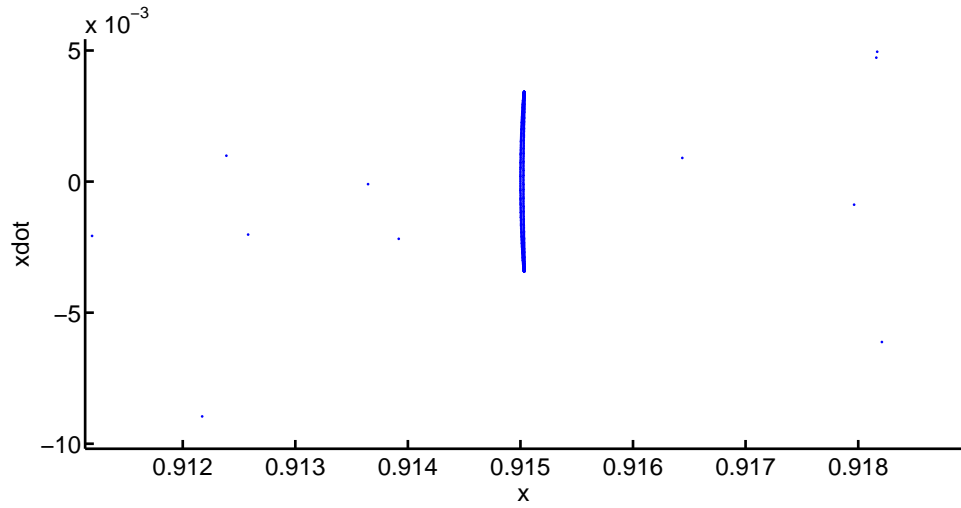


Figure 4.16: Enlarge view of PSS of second separatrix for three-loops orbit for $C = 2.96$, $A_2 = 0.0001$.

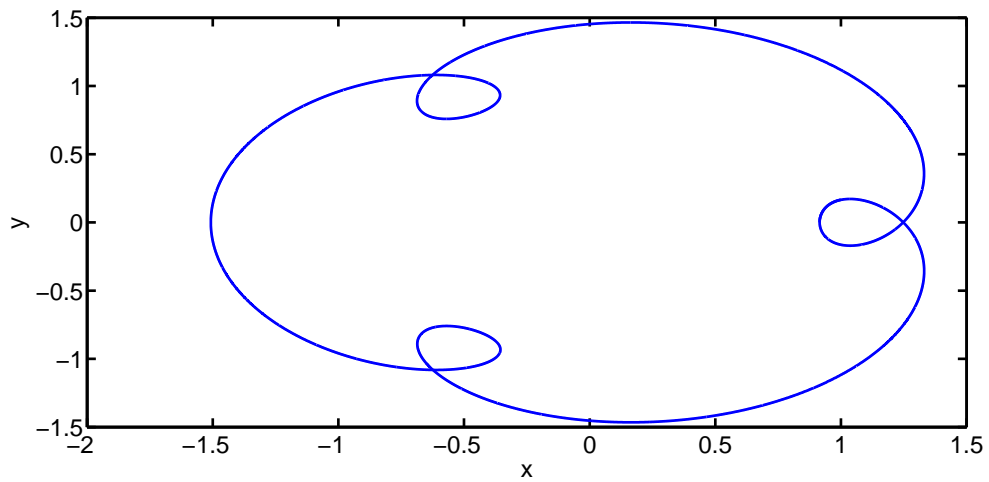


Figure 4.17: Orbit at second separatrix corresponding to $C = 2.96$, $A_2 = 0.0001$, and $x = 0.915$.

velocity (J) in the normalized dimensionless system to the dimensionalized system is given by,

$$D = R \times I, \quad (4.2.1)$$

$$V = O \times J, \quad (4.2.2)$$

where R is the distance between the centers of both primaries in km. O is the orbital velocity of second primary around first primary [Koon et. al.(2011)]. For Sun–Mars and Sun–Earth system $R = 227,940,000$ and $149,600,000$ km. respectively. Mean orbital velocity of Mars around Sun and Earth around Sun are 24.07 kms^{-1} and 29.78 kms^{-1} respectively.

It can be observed from Tables 4.5 and 4.6 that for given oblateness and given number of loops, as C decreases, V and D_1 increase while D_2 decreases. For a given C and given number of loops, as A_2 increases initial velocity and D_1 increase and D_2 decreases. So, the effect of C and oblateness A_2 is opposite in nature. For given value of A_2 and C , as number of loops increases, D_1 increases and D_2 decreases whereas V decreases up to orbits with loops 1–3 and then increases from orbits with loops 3–5.

From Table 4.5, it is observed that single–loop orbit for $A_2 = 0.00001$ is closest to Mars and the corresponding distance is 3.886×10^7 km. for $C = 2.96$. Similar notations are used in Table 4.6 also. From Table 4.6, it is observed that single–loop orbit for $A_2 = 0.00001$ is closest to Earth and this distance is 2.542×10^7 km. for $C = 2.96$. Here D_1 is the distance of secondary body from Earth.

4.3 Prediction of orbit through regression analysis

The locations of single–loop and two–loops periodic orbits obtained for different values of C and for $A_2 = 0.00001$ for Sun–Mars system is displayed in Table 4.7. Using regression analysis we have displayed the predicted position of the orbit for different values of C . The predicted and exact values of positions together with error estimates are displayed in Table 4.8. The best fit curve for single–loop is a

straight line with equation

$$x = 1.466C - 3.357$$

and the coefficient of determination $R^2 = 0.999$, whereas, for two-loops periodic orbit regression line is

$$x = 1.804C - 4.4$$

and $R^2 = 0.999$.

Similar calculations are made for single-loop and two-loops orbits for $A_2 = 0.0005$ and the relevant estimates are displayed in Tables 4.9 and 4.10. The regression curve for single-loop periodic orbit is given by

$$x = 1.9C^2 - 9.728C + 13.13$$

with $R^2 = 1$ and for two-loops periodic orbit regression curve is

$$x = 4.475C^2 - 24.56C + 34.43$$

with $R^2 = 1$. It can be observed that as C increases the error between the predicted and exact values of the position of periodic orbits increases. The PSS together with regression analysis will help one to locate the position of the periodic orbit with less effort, using the predicted positions from the analysis.

The variation of position x with respect to oblateness A_2 for Sun–Mars system for fixed value of $C = 2.96$ using PSS is shown in Table 4.11. The predicted and exact values of the position of orbits together with error estimates using regression analysis are shown in Table 4.12. For single-loop orbit the best fit regression curve is

$$x = -500.7A_2^2 - 2.5A_2 + 0.983$$

with $R^2 = 1$, whereas, for two-loops orbit

$$x = -39.14A_2^2 - 3.329A_2 + 0.941$$

with $R^2 = 1$.

The variation of position x for different values of C for single-loop and two-loops

orbit for $A_2 = 0.00001$ for Sun–Earth system is shown in Table 4.13. Using regression analysis we have displayed predicted and exact values of position together with error estimates are shown in Table 4.13. As in the case of Sun–Mars system the error estimate decreases with increase in C for both single–loop and two–loops orbits.

The best fit curve for single–loop orbit is given by

$$x = 1.466C - 3.358$$

with $R^2 = 0.999$, and for two–loops orbit regression line

$$x = 1.805C - 4.402$$

with $R^2 = 0.999$.

Similar estimates are displayed for $A_2 = 0.00005$ in Table 4.15 and Table 4.16, for Sun–Earth system. For single–loop orbit regression curve is given by

$$x = 2.125C^2 - 11.05C + 15.07$$

with $R^2 = 1$ and for two–loops orbit regression curve is given by

$$x = 4.475C^2 - 24.55C + 34.41$$

with $R^2 = 1$.

The variation of position x with oblateness A_2 for Sun–Earth system is shown in Table 4.17 for a fixed value of $C = 2.96$. The predicted and exact value of position together with error estimates are shown in Table 4.18.

The equation of the best fit curve for single–loop is

$$x = -1056A_2^2 - 2.105A_2 + 0.983$$

with $R^2 = 1$, whereas for two–loops orbit regression curve is

$$x = -58.59A_2^2 - 3.325A_2 + 0.941$$

with $R^2 = 1$.

Table 4.3: Analysis of periodic orbit for different pairs of A_2 and C for Sun–Mars system.

NL	C	$A_2 = 0.00001$			$A_2 = 0.00005$			$A_2 = 0.00010$			$A_2 = 0.00050$		
		x	L	R									
1	2.96	0.98295	0.9829	0.9830	0.98285	0.9827	0.9830	0.98272	0.9825	0.9829	0.9816	0.9815	0.9817
	2.95	0.96790	0.9678	0.9680	0.96780	0.9676	0.9680	0.96765	0.9669	0.9686	0.9666	0.9660	0.9670
	2.94	0.95324	0.9530	0.9535	0.95314	0.9530	0.9533	0.95300	0.9530	0.9530	0.95196	0.9519	0.9520
	2.93	0.93896	0.9389	0.9390	0.93887	0.9387	0.9390	0.93875	0.9386	0.9389	0.93772	0.9376	0.9378
2	2.96	0.94149	0.9406	0.9425	0.94136	0.9411	0.9414	0.94119	0.9410	0.9414	0.93985	0.9397	0.9400
	2.95	0.92251	0.9224	0.9226	0.92239	0.9223	0.9225	0.92223	0.9220	0.9225	0.92096	0.9209	0.9210
	2.94	0.90450	0.9042	0.9050	0.90438	0.9041	0.9050	0.90424	0.9040	0.9045	0.90302	0.9030	0.9030
	2.93	0.88734	0.8870	0.8878	0.88722	0.8870	0.8874	0.88708	0.8870	0.8872	0.88592	0.8858	0.8860
3	2.96	0.91529	0.9150	0.9156	0.91514	0.9150	0.9153	0.91496	0.9149	0.9150	0.91348	0.9133	0.9137
	2.95	0.89425	0.8940	0.8945	0.89412	0.8940	0.8942	0.89395	0.8939	0.8940	0.89258	0.8922	0.8930
	2.94	0.87463	0.8743	0.8748	0.87449	0.8743	0.8747	0.87433	0.8740	0.8747	0.87305	0.8730	0.8731
	2.93	0.85616	0.8560	0.8563	0.85604	0.8560	0.8561	0.85588	0.8558	0.8560	0.85467	0.8543	0.8550
4	2.96	0.89703	0.8970	0.8971	0.89688	0.8968	0.8970	0.89668	0.8965	0.8969	0.89515	0.8950	0.8953
	2.95	0.8749	0.8748	0.8750	0.87476	0.8745	0.8750	0.87458	0.8740	0.8750	0.87316	0.8730	0.8733
	2.94	0.85447	0.8544	0.8545	0.85433	0.8540	0.8547	0.85417	0.8541	0.8543	0.85284	0.8527	0.8530
	2.93	0.8354	0.8350	0.8360	0.83528	0.8350	0.8357	0.83512	0.8350	0.8353	0.83388	0.8338	0.8340
5	2.96	0.88363	0.8832	0.8834	0.88347	0.8830	0.8838	0.88328	0.8830	0.8836	0.8817	0.8814	0.8820
	2.95	0.8609	0.8608	0.8610	0.86075	0.8605	0.8610	0.86057	0.8602	0.8609	0.85912	0.8590	0.8593
	2.94	0.84004	0.8400	0.8401	0.83991	0.8398	0.8400	0.83974	0.8394	0.8401	0.83839	0.8383	0.8385
	2.93	0.82068	0.8204	0.8210	0.82056	0.8205	0.8206	0.8204	0.8200	0.8208	0.81914	0.8190	0.8193

Table 4.4: Analysis of periodic orbit for different pairs of A_2 and C for Sun–Earth system.

NL	C	$A_2 = 0.00001$			$A_2 = 0.00005$			$A_2 = 0.00010$			$A_2 = 0.00050$		
		x	L	R	x	L	R	x	L	R	x	L	R
1	2.96	0.98300	0.9830	0.9830	0.98290	0.9828	0.9830	0.98280	0.9828	0.9828	0.98170	0.9817	0.9817
	2.95	0.96790	0.9678	0.9680	0.96782	0.9676	0.9680	0.96770	0.9674	0.9680	0.96660	0.9662	0.9670
	2.94	0.95325	0.9530	0.9535	0.95315	0.9530	0.9533	0.95304	0.9530	0.9531	0.95200	0.9520	0.9520
	2.93	0.93900	0.9390	0.9390	0.93890	0.9388	0.9390	0.93877	0.9385	0.9390	0.93775	0.9375	0.9380
2	2.96	0.94155	0.9410	0.9420	0.94140	0.9410	0.9418	0.94125	0.9410	0.9415	0.93990	0.9398	0.9400
	2.95	0.92255	0.9221	0.9230	0.92244	0.9220	0.9230	0.92226	0.9220	0.9225	0.92100	0.9210	0.9210
	2.94	0.90455	0.9040	0.9051	0.90442	0.9040	0.9048	0.90426	0.9040	0.9045	0.90305	0.9030	0.9031
	2.93	0.88737	0.8870	0.8877	0.88725	0.8870	0.8875	0.88710	0.8870	0.8872	0.88595	0.8859	0.8860
3	2.96	0.91535	0.9150	0.9157	0.91520	0.9150	0.9154	0.91500	0.9150	0.9150	0.91354	0.9131	0.9141
	2.95	0.89430	0.8940	0.8946	0.89416	0.8940	0.8943	0.89400	0.8940	0.8940	0.89262	0.8922	0.8930
	2.94	0.87465	0.8743	0.87500	0.87453	0.8741	0.8750	0.87438	0.8740	0.8748	0.87309	0.8730	0.8732
	2.93	0.85620	0.8554	0.8570	0.85608	0.8560	0.8562	0.85592	0.8558	0.8560	0.85470	0.8544	0.8550
4	2.96	0.89710	0.8970	0.8972	0.89695	0.8969	0.8970	0.89675	0.8965	0.8970	0.89520	0.8950	0.8954
	2.95	0.87495	0.8749	0.8750	0.87482	0.8746	0.8750	0.87464	0.8743	0.8750	0.87321	0.8730	0.8734
	2.94	0.85450	0.8540	0.8550	0.85438	0.8540	0.8548	0.85421	0.8540	0.8544	0.85289	0.8528	0.8530
	2.93	0.83544	0.8350	0.8359	0.83532	0.8350	0.8356	0.83516	0.8350	0.8353	0.83392	0.8338	0.8340
5	2.96	0.88370	0.8834	0.8840	0.88353	0.8830	0.8841	0.88334	0.8830	0.8837	0.88175	0.8815	0.8820
	2.95	0.86095	0.8609	0.8610	0.86080	0.8606	0.8610	0.86062	0.8602	0.8610	0.85918	0.8590	0.8594
	2.94	0.84010	0.8400	0.8402	0.83995	0.8399	0.8400	0.83978	0.8396	0.8400	0.83844	0.8380	0.8389
	2.93	0.82072	0.8204	0.8210	0.82060	0.8200	0.8210	0.82044	0.8200	0.8209	0.81918	0.8190	0.8194

Table 4.5: Location, velocity and distance of orbit from both primaries for $A_2 = 0.00001, 0.00005, 0.0001, 0.0005$ for Sun–Mars system.

NL	C	$A_2 = 0.00001$			$A_2 = 0.00005$			$A_2 = 0.00010$			$A_2 = 0.00050$						
		x	$\frac{V}{\frac{km}{sec}}$	D_1 $10^7 km$	D_2 $10^8 km$	x	$\frac{V}{\frac{km}{sec}}$	D_1 $10^7 km$	D_2 $10^8 km$	x	$\frac{V}{\frac{km}{sec}}$	D_1 $10^7 km$	D_2 $10^8 km$				
1	2.96	0.98295	28.52	0.3886	2.2405	0.98285	28.53	0.3909	2.2403	0.98272	28.53	0.3938	2.2400	0.98160	28.54	0.4194	2.2374
	2.95	0.96790	28.84	0.7316	2.2062	0.96780	28.85	0.7339	2.2060	0.96765	28.85	0.7373	2.2056	0.96660	28.86	0.7613	2.2032
	2.94	0.95324	29.16	1.0658	2.1728	0.95314	29.16	1.0681	2.1725	0.95300	29.16	1.0713	2.1722	0.95196	29.18	1.0950	2.1698
	2.93	0.93896	29.48	1.3913	2.1402	0.93887	29.48	1.3933	2.1400	0.93875	29.48	1.3961	2.1397	0.93772	29.49	1.4196	2.1374
2	2.96	0.94149	28.08	1.3336	2.1460	0.94136	28.08	1.3366	2.1457	0.94119	28.08	1.3405	2.1453	0.93985	28.11	1.3710	2.1422
	2.95	0.92251	28.52	1.7662	2.1027	0.92239	28.53	1.7690	2.1024	0.92223	28.53	1.7726	2.1021	0.92096	28.55	1.8016	2.0992
	2.94	0.90450	28.96	2.1768	2.0617	0.90438	28.96	2.1795	2.0614	0.90424	28.96	2.1827	2.0611	0.90302	28.99	2.2105	2.0583
	2.93	0.88734	29.38	2.5679	2.0226	0.88722	29.39	2.5706	2.0223	0.88708	29.39	2.5738	2.0220	0.88592	29.41	2.6003	2.0193
3	2.96	0.91529	28.06	1.9308	2.0863	0.91514	28.06	1.9342	2.0859	0.91496	28.07	1.9383	2.0855	0.91348	28.10	1.9721	2.0821
	2.95	0.89425	28.59	2.4104	2.0383	0.89412	28.59	2.4134	2.0380	0.89395	28.59	2.4172	2.0376	0.89258	28.62	2.4485	2.0345
	2.94	0.87463	29.09	2.8576	1.9936	0.87449	29.09	2.8608	1.9933	0.87433	29.10	2.8645	1.9929	0.87305	29.12	2.8936	1.9900
	2.93	0.85616	29.58	3.2786	1.9515	0.85604	29.58	3.2814	1.9512	0.85588	29.58	3.2850	1.9508	0.85467	29.61	3.3137	1.9480
4	2.96	0.89703	28.15	2.3470	2.0446	0.89688	28.15	2.3505	2.0443	0.89668	28.15	2.3550	2.0438	0.89515	21.18	2.3899	2.0404
	2.95	0.87490	28.72	2.8515	1.9942	0.87476	28.72	2.8547	1.9939	0.87458	28.73	2.8588	1.9935	0.87316	28.76	2.8911	1.9902
	2.94	0.85447	29.27	3.3172	1.9476	0.85433	29.27	3.3203	1.9473	0.85417	29.27	3.3240	1.9469	0.85284	29.30	3.3543	1.9439
	2.93	0.83540	29.79	3.7518	1.9042	0.83528	29.79	3.7546	1.9039	0.83512	29.80	3.7582	1.9035	0.83388	29.82	3.7865	1.9007
5	2.96	0.88363	28.25	2.6525	2.0141	0.88347	28.25	2.6561	2.0137	0.88328	28.26	2.6605	2.0133	0.88170	28.29	2.6965	2.0097
	2.95	0.86090	28.86	3.1706	1.9623	0.86075	28.86	3.1740	1.9619	0.86057	28.86	3.1781	1.9615	0.85912	28.89	3.2112	1.9582
	2.94	0.84004	29.43	3.6461	1.9147	0.83991	29.43	3.6490	1.9144	0.83974	29.43	3.6529	1.9141	0.83839	29.46	3.6837	1.9110
	2.93	0.82068	29.98	4.0874	1.8706	0.82056	29.98	4.0901	1.8703	0.82040	29.98	4.0937	1.8700	0.81914	30.01	4.1225	1.8671

Table 4.6: Location, velocity and distance of orbit from both primaries for $A_2 = 0.00001, 0.00005, 0.0001, 0.0005$ for Sun-Earth system.

NL	C	$A_2 = 0.00001$					$A_2 = 0.00005$					$A_2 = 0.00010$					$A_2 = 0.00050$				
		x	$\frac{V}{\frac{km}{sec}}$	D_1 $10^7 km$	D_2 $10^8 km$	x	$\frac{V}{\frac{km}{sec}}$	D_1 $10^7 km$	D_2 $10^8 km$	x	$\frac{V}{\frac{km}{sec}}$	D_1 $10^7 km$	D_2 $10^8 km$	x	$\frac{V}{\frac{km}{sec}}$	D_1 $10^7 km$	D_2 $10^8 km$				
1	2.96	0.983	35.32	0.2542	1.4705	0.9829	35.32	0.2557	1.4704	0.9828	35.33	0.2572	1.4702	0.9817	35.36	0.2737	1.4686				
	2.95	0.9679	35.70	0.4801	1.4479	0.96782	35.70	0.4813	1.4478	0.9677	35.70	0.4831	1.4476	0.9666	35.72	0.4996	1.4460				
	2.94	0.95325	36.09	0.6993	1.4260	0.95315	36.09	0.7008	1.4259	0.95304	36.09	0.7024	1.4257	0.952	36.11	0.7180	1.4241				
	2.93	0.939	36.47	0.9125	1.4047	0.9389	36.47	0.9140	1.4045	0.93877	36.48	0.9159	1.4044	0.93775	36.50	0.9312	1.4028				
2	2.96	0.94155	34.75	0.8743	1.40856	0.9414	34.75	0.8766	1.4083	0.94125	34.75	0.8788	1.4081	0.9399	34.78	0.8990	1.4060				
	2.95	0.92255	35.30	1.1586	1.3801	0.92244	35.30	1.1602	1.3799	0.92226	35.30	1.1629	1.3797	0.921	35.33	1.1817	1.3778				
	2.94	0.90455	35.83	1.4278	1.3532	0.90442	35.84	1.4298	1.3530	0.90426	35.84	1.4322	1.3527	0.90305	35.87	1.4503	1.3509				
	2.93	0.88737	36.36	1.6848	1.3275	0.88725	36.36	1.6866	1.3273	0.8871	36.36	1.6889	1.3271	0.88595	36.39	1.7061	1.3253				
3	2.96	0.91535	34.72	1.2663	1.3693	0.9152	34.73	1.2685	1.3691	0.915	34.73	1.2715	1.3688	0.91354	34.77	1.2933	1.3666				
	2.95	0.8943	35.37	1.5812	1.3378	0.89416	35.37	1.5833	1.3376	0.894	35.38	1.5857	1.3374	0.89262	35.41	1.6063	1.3353				
	2.94	0.87465	35.99	1.8751	1.3084	0.87453	36.00	1.8769	1.3083	0.87438	36.00	1.8792	1.3080	0.87309	36.03	1.8985	1.3061				
	2.93	0.8562	36.60	2.1512	1.2808	0.85608	36.60	2.1529	1.2807	0.85592	36.60	2.1553	1.2804	0.8547	36.63	2.1736	1.2786				
4	2.96	0.8971	34.83	1.5393	1.34206	0.89695	34.83	1.5415	1.3418	0.89675	34.83	1.5445	1.3415	0.8952	34.87	1.5677	1.3392				
	2.95	0.87495	35.54	1.8707	1.3089	0.87482	35.54	1.8726	1.3087	0.87464	35.54	1.8753	1.3084	0.87321	35.58	1.8967	1.3063				
	2.94	0.8545	36.21	2.1766	1.2783	0.85438	36.21	2.1784	1.2781	0.85421	36.22	2.1809	1.2779	0.85289	36.25	2.2007	1.2759				
	2.93	0.83544	36.86	2.4617	1.2498	0.83532	36.86	2.4635	1.2496	0.83516	36.87	2.4659	1.2494	0.83392	36.90	2.4845	1.2475				
5	2.96	0.8837	34.95	1.7398	1.3220	0.88353	34.96	1.7423	1.3217	0.88334	34.96	1.7451	1.3214	0.88175	35.00	1.7689	1.3191				
	2.95	0.86095	35.70	2.0801	1.2879	0.8608	35.71	2.0823	1.2877	0.86062	35.71	2.0850	1.2874	0.85918	35.75	2.1066	1.2853				
	2.94	0.8401	36.41	2.3920	1.2567	0.83995	36.41	2.3943	1.2565	0.83978	36.42	2.3968	1.2563	0.83844	36.46	2.4168	1.2543				
	2.93	0.82072	37.09	2.6819	1.2278	0.8206	37.09	2.6837	1.2276	0.82044	37.10	2.6861	1.2273	0.81918	37.13	2.7050	1.2254				

Table 4.7: Variation in location of periodic orbit when $A_2 = 0.00001$ for Sun–Mars system.

NL	C	x
1	2.96	0.98295
	2.95	0.96790
	2.94	0.95324
	2.93	0.93896
2	2.96	0.94149
	2.95	0.92251
	2.94	0.90450
	2.93	0.88734

Table 4.8: Prediction and error for periodic orbit when $A_2 = 0.00001$ for Sun–Mars system.

NL	C	P_x	E_x	ER
1	2.920	0.92372	0.92508	0.00136
	2.925	0.93105	0.93198	0.00093
	2.935	0.94571	0.94605	0.00034
	2.945	0.96037	0.9605	0.00013
	2.955	0.97503	0.9754	0.00037
	2.965	0.98969	0.99069	0.001
2	2.920	0.86768	0.87092	0.00324
	2.925	0.8767	0.87904	0.00234
	2.935	0.89474	0.89582	0.00108
	2.945	0.91278	0.9134	0.00062
	2.955	0.93082	0.931875	0.001055
	2.965	0.94886	0.9514	0.00254

Table 4.9: Variation in location of periodic orbit when $A_2 = 0.0005$ for Sun–Mars system.

NL	C	x
1	2.96	0.98160
	2.95	0.96660
	2.94	0.95196
	2.93	0.93772
2	2.96	0.93985
	2.95	0.92096
	2.94	0.90302
	2.93	0.88592

Table 4.10: Prediction and error for periodic orbit when $A_2 = 0.0005$ for Sun–Mars system.

NL	C	P_x	E_x	ER
1	2.920	0.924400	0.923870	-0.00053
	2.925	0.931288	0.930750	-0.00054
	2.935	0.945348	0.944800	-0.00055
	2.945	0.959787	0.959220	-0.00057
	2.955	0.974607	0.974040	-0.00057
	2.965	0.989808	0.989290	-0.00052
2	2.920	0.870440	0.869550	-0.00089
	2.925	0.878422	0.879040	0.000618
	2.935	0.895057	0.895820	0.000763
	2.945	0.912587	0.913400	0.000813
	2.955	0.931012	0.931875	0.000860
	2.965	0.950332	0.951400	0.001068

Table 4.11: Variation in location of periodic orbit when $C = 2.96$ for Sun–Mars system.

NL	A_2	x
1	0.00001	0.98295
	0.00005	0.98285
	0.00010	0.98272
	0.00050	0.98160
2	0.00001	0.94149
	0.00005	0.94136
	0.00010	0.94119
	0.00050	0.93985

Table 4.12: Prediction and error for periodic orbit when $C = 2.96$ for Sun–Mars system.

NL	A_2	P_x	E_x	ER
1	0.000025	0.982937187	0.982930	-7.1870×10^{-6}
	0.000075	0.982809684	0.98280	-9.6830×10^{-6}
	0.000250	0.982343706	0.98233	-1.3706×10^{-5}
	0.000750	0.980843356	0.98095	1.0664×10^{-4}
2	0.000025	0.940916751	0.94145	0.000533249
	0.000075	0.940750105	0.94128	0.000529895
	0.000250	0.940165304	0.94069	0.000524696
	0.000750	0.938481234	0.93902	0.000538766

Table 4.13: Variation in location of periodic orbit when $A_2 = 0.00001$ for Sun–Earth system.

NL	C	x
1	2.96	0.98300
	2.95	0.96790
	2.94	0.95325
	2.93	0.93900
2	2.96	0.94155
	2.95	0.92255
	2.94	0.90455
	2.93	0.88737

Table 4.14: Prediction and error for periodic orbit when $A_2 = 0.00001$ for Sun–Earth system.

NL	C	P_x	E_x	ER
1	2.920	0.922720	0.92510	0.00238
	2.925	0.930050	0.93200	0.00195
	2.935	0.944710	0.94610	0.00139
	2.945	0.959370	0.96055	0.00118
	2.955	0.974030	0.97542	0.00139
	2.965	0.988690	0.99072	0.00203
2	2.920	0.868600	0.87095	0.00235
	2.925	0.877625	0.87909	0.001465
	2.935	0.895675	0.89588	0.000205
	2.945	0.913725	0.91342	-0.00030
	2.955	0.931775	0.93190	0.000125
	2.965	0.949825	0.95147	0.001645

Table 4.15: Variation in location of periodic orbit when $A_2 = 0.0005$ for Sun–Earth system.

NL	C	x
1	2.96	0.98170
	2.95	0.96660
	2.94	0.95200
	2.93	0.93775
2	2.96	0.94140
	2.95	0.92244
	2.94	0.90442
	2.93	0.88725

Table 4.16: Prediction and error for periodic orbit when $A_2 = 0.0005$ for Sun–Earth system.

NL	C	P_x	E_x	ER
1	2.920	0.922600	0.92501	0.002410
	2.925	0.929453	0.93189	0.002437
	2.935	0.943478	0.94599	0.002512
	2.945	0.957928	0.96044	0.002512
	2.955	0.972803	0.97532	0.002517
	2.965	0.988103	0.99062	0.002517
2	2.920	0.879640	0.87083	-0.00881
	2.925	0.887672	0.87896	-0.00871
	2.935	0.904407	0.89573	-0.00868
	2.945	0.922037	0.91333	-0.00871
	2.955	0.940562	0.93180	-0.00876
	2.965	0.959982	0.95130	-0.00868

Table 4.17: Variation in location of periodic orbit when $C = 2.96$ for Sun–Earth system.

NL	A_2	x
1	0.00001	0.98300
	0.00005	0.98290
	0.00010	0.98280
	0.00050	0.98170
2	0.00001	0.94155
	0.00005	0.94140
	0.00010	0.941250
	0.00050	0.93990

Table 4.18: Prediction and error for periodic orbit when $C = 2.96$ for Sun–Earth system.

NL	A_2	P_x	E_x	ER
1	0.000025	0.982946715	0.98294	-6.715×10^{-6}
	0.000075	0.982836185	0.98283	-6.185×10^{-6}
	0.000250	0.98240775	0.98240	-7.750×10^{-6}
	0.000750	0.98082725	0.98100	1.7275×10^{-4}
2	0.000025	0.940916838	0.94150	0.000583162
	0.000075	0.940750295	0.94133	0.000579705
	0.000250	0.940165088	0.94074	0.000574912
	0.000750	0.938473293	0.93906	0.000586707

4.4 Conclusion

In this chapter, we have studied the effect of oblateness on the position, shape and size of closed periodic orbits with loops varying from 1 to 5 for Sun–Mars and Sun–Earth systems, respectively. It is concluded that for given number of loops and given C , as oblateness increases, location of periodic orbit moves towards Sun. For given C and given oblateness, as number of loops increases, location of periodic orbits shift towards Sun. For given value of oblateness and given number of loops, as C decreases, location of periodic orbit moves towards Sun. Also, period of the orbit increases as number of loops increases. It is also observed that single–loop orbit is closest to second primary body. Further, as number of loops decreases, width of the orbit increases.

The distance of closest approach of the secondary body from the smaller primary increases with oblateness and number of loops for a given C . Thus, the present analysis of the two systems–Sun–Mars and Sun–Earth systems–using PSS technique reveals that A_2 and C has substantial effect on the position, shape and size of the orbit. The PSS together with regression analysis will help one to locate the position of the periodic orbit with less effort, using the predicted positions from the analysis. It can be observed that for given oblateness and given number of loops, as Jacobi constant decreases, initial velocity of secondary body (spacecraft) and distance of spacecraft from second primary increase and distance of spacecraft from first primary body decreases. For given Jacobi constant and given number of loops, as oblateness increases, initial velocity increases and distance of spacecraft from second primary increases and the distance of spacecraft from first primary decreases. Thus, the effect of Jacobi constant C and oblateness coefficient A_2 is opposite in nature. For given value of oblateness coefficient and Jacobi constant, as number of loops increases, distance of spacecraft from second primary increases and distance of spacecraft from first primary decreases whereas initial velocity of the spacecraft decreases for orbits from single–loop to three–loops and then increases for orbits from 3–loops to 5–loops. It is further observed that for Sun–Mars system, single–loop orbit for $A_2 = 0.00001$ and $C = 2.96$ is closest to Mars and this distance is 3.886×10^7 km. For Sun–Earth system, single–loop orbit for $A_2 = 0.00001$ and $C = 2.96$ is closest to Earth and this distance is 2.542×10^7 km. Since stability of this class of periodic orbits is very low, it can be used for designing low–energy

trajectory design for space mission.